



HAL
open science

Mass Transfer Rate Parameters of Sulzer EX Laboratory Scale Gauze Structured Packing

John Roesler, Arslan Muhammad

► **To cite this version:**

John Roesler, Arslan Muhammad. Mass Transfer Rate Parameters of Sulzer EX Laboratory Scale Gauze Structured Packing. *Chemical Engineering Transactions*, 2018, 69, pp.55-60. hal-01900575

HAL Id: hal-01900575

<https://ifp.hal.science/hal-01900575>

Submitted on 22 Oct 2018

HAL is a multi-disciplinary open access archive for the deposit and dissemination of scientific research documents, whether they are published or not. The documents may come from teaching and research institutions in France or abroad, or from public or private research centers.

L'archive ouverte pluridisciplinaire **HAL**, est destinée au dépôt et à la diffusion de documents scientifiques de niveau recherche, publiés ou non, émanant des établissements d'enseignement et de recherche français ou étrangers, des laboratoires publics ou privés.

Mass Transfer Rate Parameters of Sulzer EX Laboratory Scale Gauze Structured Packing

John Roesler*, Arslan Muhammad

IFP Energies Nouvelle, Solaize 69360, France
john.roesler@ifpen.fr

Sulzer EX packing is widely used in lab-scale separation studies owing to its high efficiency, low theoretical stage height and small pressure drop. In this work the three fundamental characteristic mass transfer parameters of this packing, effective gas-liquid contact area (a_e) gas-film and liquid-film mass transfer coefficient (k_G) and (k_L) are measured in a 0.19 mm ID counter-flow absorption column using aqueous liquids. With end effects removed, the results show that the effective gas liquid contact area is independent of gas and liquid loads and reaches about 90 % of the geometric area of the packing. Correlations of the dimensionless gas and liquid phase mass transfer parameters are determined as $Sh_G = 0.048 Re_G^{1.0} Sc_G^{0.33}$ and $Sh_L = 0.050 Re_L^{0.4} Sc_L^{0.5}$.

1. Introduction

Structured packings are well known devices used in separation columns since they offer excellent capacity per efficiency unit and low pressure drop. The Sulzer EX structured packing is widely used for lab scale separation studies owing to its high geometric area, a_g of $1700 \text{ m}^2/\text{m}^3$, and gauze-type nature which results into high efficiency with low pressure drop. The gauze elements (or blocks) operate typically on a fully wetted basis, even under high vacuum conditions, ensuring low resistance to mass transfer (Bravo et al., 1985). This type of packing is particularly suitable for operations where a large number of theoretical stages is required. Others have also found that Sulzer EX, for CO_2 absorption in post-combustion processes, provides an excellent overall mass transfer coefficient which is higher than for random packings by a factor of 10 to 33 (Tontiwachwuthikul and Aroonwilas, 1997). However, despite the frequent use of this packing little information has been reported on its mass-transfer properties in terms of the gas-and liquid-side mass transfer coefficients and the interfacial areas for gas-liquid contact. These parameters are of fundamental importance for the use of rate-based models to size separation columns or to analyse data. The present work provides measurements of the three fundamental mass transfer parameters, k_L , k_G and a_e for the EX packing with aqueous liquids.

2. Experimental facility and protocol

The experimental facility is shown schematically in Figure 1. It consists in a lab-scale glass shell and tube type column with an inner diameter of 0.019 m and a total column height of 1 m capable of a maximum packed height of 0.72 m. The packing elements were 0.054 m tall with a 0.017 mm diameter. Operation was in counter-current mode. The liquid solvent was pumped from a storage tank through a centrifugal pump to the top of the column and distributed by a single drip-tube. The inlet gas stream composition was set by mixing the metered flows from various gas bottle mixtures. Gas samples were taken either from the inlet or the outlet lines which were connected to the gas analyser through thermostatically controlled sample lines at 45°C to avoid any condensation. A liquid coolant was introduced from the shell side of the column to hold the column at the desired temperature. Prior to each experiment, the packing was repeatedly flooded with the solvent then drained to produce packing surfaces that were clean and readily wetted. Since no liquid flow was observed at the walls, the gas superficial velocity was calculated using the column diameter while the liquid superficial velocity was calculated with the packing diameter.

2.1 Effective gas-liquid contact area (a_e) measurements

The effective gas-liquid contact area of the packing is measured by the absorption of atmospheric carbon dioxide with a 0.1 gmol/L sodium hydroxide solution. This method has been widely used in the literature to measure the effective area of various packings (Hegeley et al. 2017).

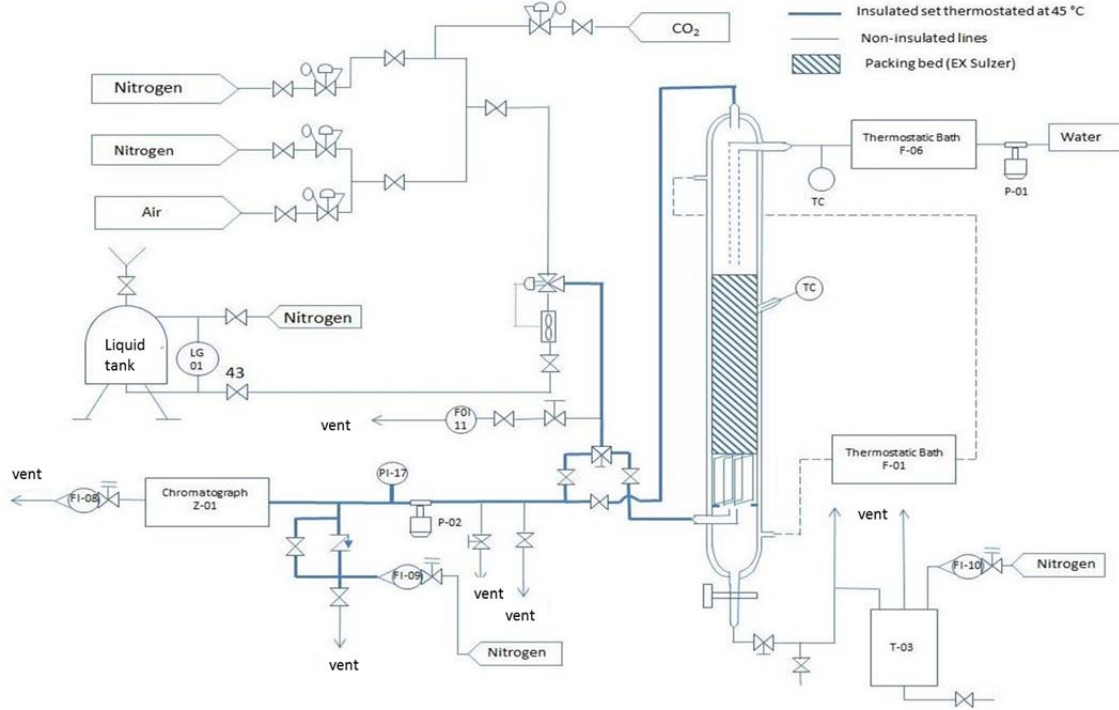


Figure 1: Schematic diagram of the experimental facility.

A first set of measurements was taken with one block of packing. In a typical experiment, 0.01 m³ of 0.1 gmol/L NaOH solution were prepared in the storage tank. The initial NaOH concentration was measured by manual titration. A Rosemount® NGA-200 carbon dioxide analyser was used to evaluate inlet and outlet CO₂ concentrations. Three gas superficial velocities of (0.6, 1, 1.3 m/s) and four superficial liquid velocities (1.6, 3.3, 6.6 and 12.5 m/h) were used for a typical gas-liquid contact area study. The column temperature and pressure were kept at 10 °C and 1 bar respectively. The inlet and outlet CO₂ concentrations were measured sequentially after the system had reached steady state. With the inlet and outlet CO₂ concentration known, the effective area was calculated with equation (6). Test runs were completed first with one block of packing, then with two or more.

The effective area is calculated from the overall volumetric mass transfer given by as:

$$K_{OG}a_e = \frac{u_G}{Z} NTU_{OG} \quad (1)$$

With

$$NTU_{OG} = \int_{out}^{in} \left(\frac{1}{y_i - y_i^*} \right) dy_i \quad (2)$$

where K_{OG} (m/s) is the overall volumetric mass transfer coefficient, NTU_{OG} is the number of transfer units, u_G (m/s) is the gas superficial velocity and Z (m) is the packed bed height, y_i is the solute mole fraction in the gas phase and y_i^* is solute gas mole fraction at equilibrium with the bulk liquid. With the present system, at low loadings, $y_{CO_2}^*$ is negligible such that:

$$NTU_{OG} = \ln \left(\frac{y_{CO_2,in}}{y_{CO_2,out}} \right) \quad (3)$$

According to the two-film theory (Danckwerts, 1970), the overall mass transfer resistance when a reaction is taking place in the liquid film is:

$$\frac{1}{K_{OG}} = \frac{1}{k_G} + \frac{He/RT}{E k_L} \quad (4)$$

Where He is Henry's law coefficient (Pa/(mol/m³)), k_G and k_L (m/s) are the gas and liquid film mass transfer coefficients respectively, E is the enhancement factor from the chemical reaction, R is the gas constant and T the temperature. When CO₂ partial pressures are low, and hydroxide ions are present in relative excess, the reaction can be treated as pseudo-first-order irreversible in the fast regime (Danckwerts, 1970) such that:

$$E = Ha = \frac{\sqrt{k_{OH^-}[OH^-] D_{CO_2,liq}}}{k_L} \quad (5)$$

Where $D_{CO_2,liq}$ is the diffusivity coefficient (m²/s), k_{OH^-} is the pseudo-first-order rate constant (s⁻¹) and $[OH^-]$ is the concentration of anions (mol/m³). Combining equations (1) to (5) finally leads to:

$$a_e = \left(\frac{1}{k_G} + \frac{He/RT}{\sqrt{k_{OH^-}[OH^-] D_{CO_2,liq}}} \right) \frac{u_G \cdot NTU_{OG}}{Z} \quad (6)$$

The liquid loading in carbonates does not exceed 5% along the column so the solution properties are assumed constant and equal to those of the neat solution. The kinetic parameters of the reaction were taken from Pohorecki and Moniuk (1988). In many cases the gas side resistance to mass transfer can be neglected with this system (e.g. Alix et al. 2011). In the present case, k_G measurements show that this resistance contributes to between 10 and 16% of the total. It is also important to assess that the chemical system is in the proper regime. In the present case, with very low values of k_L , the system might be too close to the instantaneous regime where the acceleration factor reaches its maximum value E_i . Criteria are mentioned in the review of Hegely et al. (2017), the most severe of which is $E_i/Ha > 5$. In our experiments the values ranged from 4 to 10, so the criterion is met except at the lowest liquid loads where k_L is smallest. The criterion for $E = Ha$ is also met since $Ha > 4$ in all cases.

In order to calculate the effective area of the EX packing for fully developed flowfield, the results obtained with one packing element, which inherently contain all end effects, are removed from those with two elements by using the additivity of transfer units:

$$(NTU_{OG})_{2 \text{ blocks}} = (NTU_{OG})_{1st \text{ block}} + (NTU_{OG})_{2nd \text{ block}} \quad (7)$$

Applying equation (5) then gives:

$$(a_e Z)_{2 \text{ blocks}} = (a_e Z)_{1st \text{ block}} + (a_e Z)_{2nd \text{ block}} \quad (8)$$

And finally

$$a_{e,net} = 2(a_e)_{2 \text{ blocks}} - (a_e)_{1st \text{ block}} \quad (9)$$

2.2 Gas phase film mass transfer coefficient (k_G) measurement

The gas phase film mass transfer coefficient is measured by the absorption of sulphur dioxide diluted with nitrogen into a 2 N sodium hydroxide solution which is a commonly used system (e.g. Rejl et al. 2009, Wang et al. 2016). The reaction between SO₂ and NaOH is an instantaneous reaction, making the liquid phase resistance negligible. The gas phase film mass transfer coefficient can then be calculated by the following equation:

$$k_G a_e = \frac{u_G}{Z} \ln \left(\frac{y_{SO_2,in}}{y_{SO_2,out}} \right) \quad (10)$$

It was not possible to make measurements with two packing elements as the outlet SO₂ concentrations were then below detection limit. The range of gas superficial velocities investigated went from 0.05 to 0.15 m/s at two liquid superficial velocities of 3.5 to 10 m/h. The inlet SO₂ concentrations ranged from 0.1 to 0.3 %vol. The column was operated at 10 °C and atmospheric pressure. The gas phase sample of the inlet and outlet were pumped to the SO₂ analyser (Horiba® VA-3000).

End effects were accounted for by making measurements with no packing element to calculate NTU_B , the number of transfer units of the empty column. The effective area obtained from using one packing element was used to get the gas phase mass transfer coefficient:

$$k_G = \frac{u_G}{(a_e Z)_{1st\ block}} \left(\ln \left(\frac{y_{SO_2, in}}{y_{SO_2, out}} \right) - NTU_B \right) \quad (11)$$

2.3 Liquid phase film mass transfer coefficient (k_L) measurement

The liquid film mass transfer coefficient was measured through the physical absorption into water of acetaldehyde vapour (MeCHO) diluted with nitrogen. Experiments were performed at 20°C and atmospheric pressure with 1 and 2 elements of packing. The liquid superficial velocities ranged from 1 to 3.7 m/h while only two superficial gas velocities of 0.48 and 1.0 m/s were investigated since k_L is weekly dependent on gas flowrate. The inlet gas mixture was prepared by vaporizing a pure liquid acetaldehyde solution into a stream of nitrogen to reach column inlet concentrations in the range of 0.5 to 0.8 %vol. A Gas Chromatograph connected on-line was used to measure the steady-state inlet and outlet acetaldehyde concentrations.

With a non-reactive system, the two-film theory simplifies to:

$$\frac{1}{K_{OG}} = \frac{1}{k_G} + \frac{He/RT}{k_L} \quad (12)$$

Under the conditions tested, the gas side resistance contributes from 16 to 35% of the total. Furthermore MeCOH accumulates rapidly in the liquid phase such that its equilibrium partial pressure is not negligible. Therefore a full 1-D absorption model that uses knowledge of k_G and a_e from above was required to determine k_L by regression to match experimental and calculated gas outlet MeCOH concentrations. The model molar flux (moles/s/m³) is given by:

$$\varphi_i(z) = K_{OG}(z) a_e(z) (y_i(z) - y_i^*(z)) \frac{P}{RT} \quad (13)$$

where z is the distance along the column. The model takes into account entrance effects by associating a height dependence to K_{OG} and a_e , with a specific set of values for the first element of packing and another set for all subsequent elements. The thermodynamic properties were constant since temperature and pressure do not vary. Gas and liquid flow velocity variations were neglected.

3. Results and discussion

The effective area is found to be nearly constant with no significant dependence either on gas or liquid flow rates. Figure 2a shows the fractional areas, a_e/a_g , measured for beds of 1 and 2 elements of packing. The lower values for the first packing element indicates that entrance liquid distribution lowers effective area, which is expected since the fluid enters through a single drip point. When this end effect is taken into account the net fractional area values shown in Figure 2b reach values of 0.90 within $\pm 2.5\%$, thus only 10 % below a fully wetted packing. Figure 2b also shows a negligible dependence of effective area on gas and liquid flowrates. These features can be explained by the woven nature of the packing material which gives good wetting and constrains the fluid to a smooth homogeneous laminar flow. Some investigators have assumed gauze packings to be fully wetted with $a_e/a_g = 1.0$ (Zogg, 1973, Bravo et al., 1985). This behaviour contrasts with those of plain metal sheet structured packings which have effective areas that depend on liquid velocity to the power 0.15 (Wang et al. 2016) due to less efficient wetting at low liquid loads. The incomplete wetting observed here could be due to partial channel blockage owing to the high surface tension of aqueous systems.

The measured gas film mass transfer coefficients, k_G , are presented in Figure 3 where the values show a linear dependency to gas velocity but are independent of liquid load, as typically observed structured packings operating below the loading point. An empirical dimensionless correlation is determined as:

$$Sh_G = 0.048 Re_G^{1.0} Sc_G^{0.33} \quad (14)$$

with the dimensionless groups defined on the same basis as Wang (2015):

$$Sh_G = \frac{k_G}{D_{i,G} a_g}, \quad Re_G = \frac{u_G}{v_G a_g}, \quad Sc_G = \frac{D_{i,G}}{v_G} \quad (15)$$

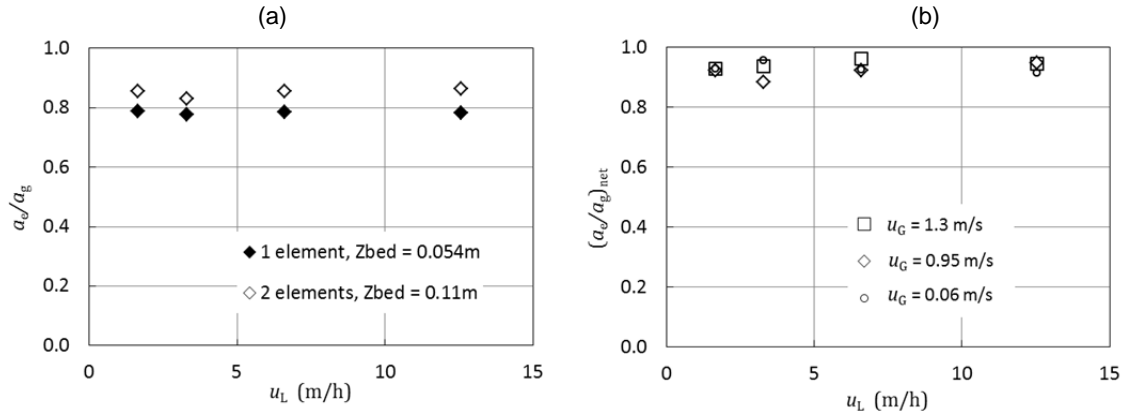


Figure 2: Measured fractional areas (a) brut values at different bed heights and (b) net values at varying gas superficial velocities.

where $D_{i,G}$ is the solute diffusivity in the gas phase, ν_G is the gas phase kinematic viscosity. With these definitions the characteristic dimension is taken as $1/a_g$ which is representative of the hydraulic diameter of a channel formed by the packing corrugations. The exponent on Sc_G is taken from the literature as a common value for structured packings. The exponent on Re_G is similar to the values found in the literature for Sulzer CY and BX or Montz-A2 gauze-type structured packings that fall between 0.8 and 1.0 (Weiland and Kelly (1993), Zogg (1973), Bravo et al. (1985)).

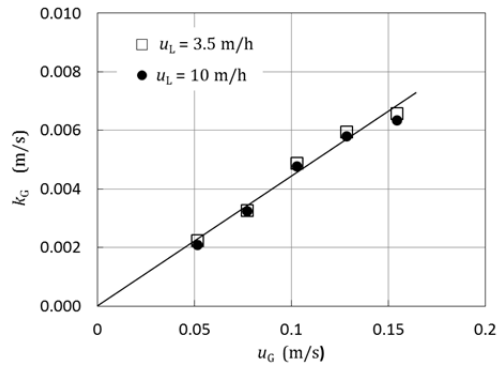


Figure 3: Gas phase film mass transfer coefficient k_G as a function of gas superficial velocity. The line is a linear curve fit.

The regressed values of k_L are shown in Figure 4a as a function of liquid load, while Figure 4b is a parity plot comparing the measured and calculated exit unabsorbed fraction of injected solute ($y_{i,out}/y_{i,in}$). The top element of packing has the highest k_L which is likely due to the higher entrance film velocities. The second and subsequent layers of packing have a k_L that is 2.5 times lower. The measurements with one and two packing elements served to determine the k_L correlations. For these bed heights the parity plot therefore shows the best agreement, within better than 10%. The empirical dimensionless correlation for the second and subsequent packing layers is determined as:

$$Sh_L = 0.050 Re_L^{0.4} Sc_L^{0.5} \quad (16)$$

with the dimensionless groups defined on the same basis as equation (15) but with the liquid properties and superficial velocity. The correlation for the top packing layer was the same but for a 2.5 times higher proportionality coefficient. The power coefficient on Sc_L is taken from the literature as a common value for structured packings. The coefficient on Re_L leads to a dependency to u_L to the power 0.4 which is close to the value of 0.5 given by the Higbie penetration theory, as noted in Bravo et al. (1985).

The model was then used with these correlations to simulate results of longer beds up to 0.65 m under similar flow conditions. The parity plot shows less good yet satisfactory results for these longer beds with some points spreading to 25% disagreement.

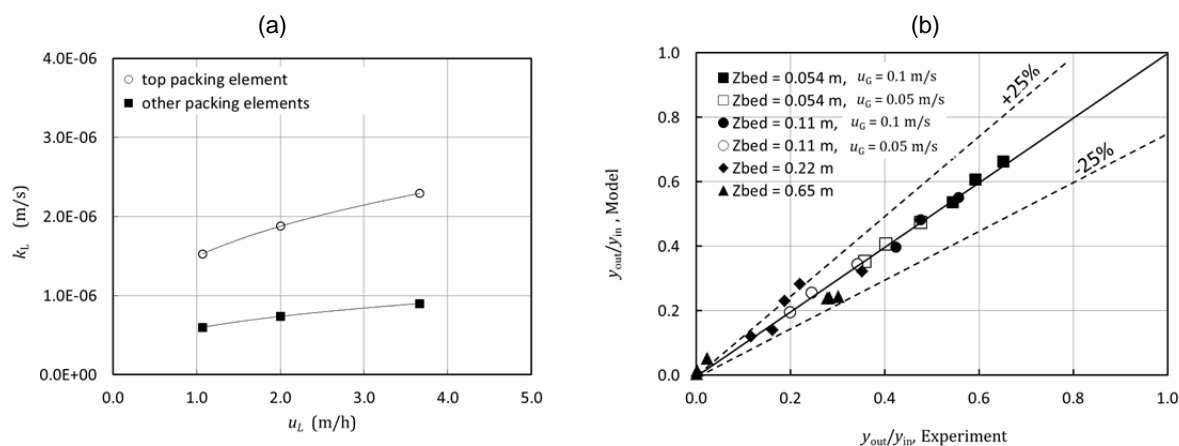


Figure 4: k_L regression results: (a) liquid film mass transfer coefficient at the three experimental liquid flowrates and (b) parity plot of the exit solute mole fraction.

4. Conclusions

Three fundamental mass transfer properties for Sulzer EX packing have been determined: effective gas-liquid contact area (a_e), gas-film mass transfer coefficient (k_G), and liquid-film mass transfer coefficient (k_L). With end effects properly taken into account, the intrinsic effective areas are found to be close to the packing geometric area and independent of liquid and gas loads with $a_e/a_g=0.9$. This result is coherent with the woven nature of the packing material that allows good wetting by capillary action under all conditions. The incomplete wetting could be due to partial channel blockage due to the high surface tension of aqueous systems. The dimensionless gas and liquid phase film mass transfer coefficients were also evaluated with end effects removed. They show classical power law dependencies to the associated Reynolds numbers: $Sh_G \sim Re_G^{1.0}$, $Sh_L \sim Re_L^{0.4}$. The magnitudes of the exponents are typical for structured packing. The mass transfer parameter correlations were developed from one and two packing elements and successfully applied to simulate physical absorption rates of acetaldehyde into water within 25% for bed heights of up to 11 packing elements (0.65 m). These correlations will be useful for the design and modeling of future laboratory columns using this packing.

References

- Alix P., Raynal L., Abbe F., Meyer M., Prevost M., Rouzineau D., 2011, Chem. Eng. Res. Des., 89 (9):1658–1668.
- Bravo L., Rocha J. A., Fair J. R., 1985. Mass transfer in gauze packings, Hydrocarbon Process, 64 (1) 91-5.
- Danckwerts P.V., 1970, Gas-Liquid Reactions. New York: McGraw-Hill Book Company.
- Hegely L., Roesler J., Pascal A., Rouzineau D., Meyer M., 2017, Absorption methods for the determination of mass transfer parameters of packing internals: A literature review, AIChE J., vol. 63, no. 8, p. 3246–3275.
- Pohorecki, R. and Moniuk W., 1988, Kinetics of reaction between carbon-dioxide and hydroxyl ions in aqueous-electrolyte solutions, Chem. Eng. Sci., 43 (7), 1677-1684.
- Rejl J.F., Linek V., Moucha T., Valenz L., 2009, Methods standardization in the measurement of mass-transfer characteristics in packed absorption columns, Chem. Eng. Res. Des. 87, 695–704.
- Tontiwachwuthikul P., Aroonwilas A., 1997, High-efficiency structured packing for CO₂ separation using 2-amino-2-methyl-1-propanol (AMP), Sep. Purif. Technol., 12, 67–79.
- Wang C., Song D., Seibert F. A., Rochelle G. T., 2016, Dimensionless models for predicting the effective area, liquid-film, and gas-film mass-transfer coefficients of packing, Ind. Eng. Chem. Res., 55, 5375-5384.
- Weiland R. H., Kelly R. A., 1993, Mass transfer characteristics of some structured packings, Ind. Eng. Chem. Res., 32, 1411-1418.